T.C.
BAHCESEHIR UNIVERSITY
GRADUATE SCHOOL
THE DEPARTMENT OF MECHATRONICS ENGINEERING
MASTER PROGRAM IN MECHATRONICS ENGINEERING BAU-AKINROBOTICS ARTIFICIAL INTELLIGENCE AND ROBOTIC TECHNOLOGY

PATH PLANNING FOR A SURGICAL ROBOTIC ARM USING AN UPGRADED RRT STAR ALGORITHM

MASTER'S THESIS

MARIE DAMIEN NDZENGUE MEBEBE

ISTANBUL 2025

T.C.
BAHCESEHIR UNIVERSITY
GRADUATE SCHOOL
THE DEPARTMENT OF MECHATRONICS ENGINEERING
MASTER PROGRAM IN MECHATRONICS ENGINEERING, BAU-AKINROBOTICS ARTIFICIAL INTELLIGENCE AND ROBOTICS TECHNOLOGY

PATH PLANNING FOR A SURGICAL ROBOTIC ARM USING AN UPGRADED RRT STAR ALGORITHM

MASTER'S THESIS

MARIE DAMIEN NDZENGUE MEBEBE

THESIS ADVISOR

ASSIST. PROF. BESTE BAHÇECI

ISTANBUL 2025

T.C.
BAHCESEHIR UNIVERSITY
GRADUATE SCHOOL

21/05/2025

MASTER THESIS APPROVAL FORM

Program Name:	MECHATRONICS ENGINEERING (ENGLISH, THESIS), BAU-AKINROBOTICS ARTIFICIAL INTELLIGENCE AND ROBOTIC TECHNOLOGIES
Student's Name and Surname:	MARIE DAMIEN NDZENGUE MEBEBE
Name Of The Thesis:	PATH PLANNING FOR A SURGICAL ROBOTIC ARM USING AN UPGRADED RRT STAR ALGORITHM
Thesis Defense Date:	21/05/2025

This thesis has been approved by the Graduate School which has fulfilled the necessary conditions as Master thesis.

Assoc. Prof. Yücel Batu SALMAN
Director of Graduate School

This thesis was read by us, quality and content as a Master's thesis have been seen and accepted as sufficient.

	Title, Name	**Institution**	**Signature**
Thesis Advisor:	Asst. Prof. Beste Bahçeci	Bahçeşehir University	
2nd Member	Asst. Prof. Senem Seven	Bahçeşehir University	
3rd Member (Outside Institution)	Asst. Prof. Ahmet Fatih Tabak	Istanbul Ticaret University	

I hereby declare that all information in this document has been obtained and presented in accordance with academic rules and ethical conduct. I also declare that, as required by these rules and conduct, I have fully cited and referenced all material and results that are not original to this work.

Name, Last Name: Marie Damien Ndzengue M.

Signature:

ABSTRACT

PATH PLANNING FOR A SURGICAL ROBOTIC ARM USING AN UPGRADED RRT STAR ALGORITHM

Marie Damien Ndzengue Mebebe

Master Program in Mechatronics Engineering, Bau-Akinrobotics Artificial Intelligence And Robotic Technologies

Thesis Advisor: Assist. Prof. Beste Bahçeci

May 2025, 34 pages

Robot-assisted surgery demands reliable trajectory planning to safely and efficiently navigate the complexities of the anatomical environment. Although real-time adaptive path planning has been extensively explored, offline path planning remains indispensable for preoperative procedures, offering robust, well-defined trajectories before surgical execution. A broad spectrum of path planning algorithms has been developed, each tailored to specific application domains and desired outcomes. Among these, Rapidly exploring Random Tree (RRT) and its variants are widely utilised in medical robotics. However, they continue to suffer from significant limitations, such as extended computation time and the generation of unfeasible or non-smooth trajectories. This study introduces an upgraded version of RRT star (U-RRT*) designed to overcome these shortcomings and improve the overall effectiveness of path planning. The proposed approach optimises the sampling strategy by directing it towards the goal, thereby reducing computation time. Additionally, it integrates a clearance threshold mechanism to ensure safe navigation around anatomical obstacles. To further enhance path quality, the method employs B-spline interpolation in conjunction with a rotation matrix, resulting in smooth, continuous and Jerk-free trajectories.

Key Words: RRT Algorithm, Offline Path Planning, Sampling-based Planning, B-spline Smoothing.

ÖZET

GELİŞTİRİLMİŞ RRT* ALGORİTMASI KULLANILARAK CERRAHI ROBOTİK KOL İÇİN YOL PLANLAMASI

Marie Damien Ndzengue Mebebe
Bau-Akinrobotics Yapay Zeka Ve Robotik Teknolojileri Mekatronik Mühendisliği Yüksek Lisans Programı
Tez Danışmanı: Dr. Öğr. Üyesi Beste Bahçeci

Mayıs 2025, 34 sayfa

Robot destekli cerrahi, anatomik yapıların karmaşıklığı içerisinde güvenli ve etkili bir şekilde gezinmeyi sağlamak için son derece güvenilir bir yörünge planlamasına ihtiyaç duyar. Gerçek zamanlı uyarlamalı yol planlama kapsamlı bir şekilde araştırılmış olsa da, cerrahi öncesi süreçlerde sağlam ve iyi tanımlanmış yörüngeler sunması açısından çevrimdışı yol planlama hâlâ vazgeçilmezdir. Günümüzde, belirli uygulama alanlarına ve hedeflenen sonuçlara göre uyarlanmış çok çeşitli yol planlama algoritmaları geliştirilmiştir. Bu algoritmalar arasında, Rapidly-exploring Random Tree (RRT) ve türevleri, tıbbi robotikte yaygın olarak kullanılmaktadır. Ancak bu algoritmalar, uzun hesaplama süreleri ve uygulanabilir olmayan ya da düzgün olmayan yollar üretmeleri gibi önemli kısıtlarla karşı karşıyadır.

Bu çalışma, söz konusu eksiklikleri gidermek ve yörünge planlamasının genel etkinliğini artırmak amacıyla geliştirilmiş bir RRT* algoritması önermektedir. Önerilen yaklaşım, örnekleme stratejisini hedefe yönlendirerek planlama süresini azaltır. Ayrıca, anatomik çevrelerde sıkça karşılaşılan engellerin güvenli bir şekilde aşılmasını sağlamak üzere bir açıklık eşik mekanizması entegre edilmiştir. Yörünge kalitesini daha da artırmak için yöntem, B-spline enterpolasyonu ile birlikte bir dönüşüm matrisi kullanarak düzgün, kesintisiz ve sarsıntısız yollar üretir.

Anahtar Kelimeler: RRT Algorithm, Offline Path Planning, Sampling-based Planning, B-spline Smoothing.

To my Lovely Family and Friends who rendered this journey possible and amazing with their support.

ACKNOWLEDGEMENTS

I wish to express my deepest gratitude to my supervisor, Dr. Beste Bahçeci, for her guidance, advice, criticism, encouragement and insight throughout the research.

I would also like to thank my parents, Jean Michel Mebebe and Dorothee Odzomo, for their great support throughout my academics. Without their understanding and continuous support, I could have never been able to aspire to this level of education and complete this study.

TABLE OF CONTENTS

LIST OF TABLES

TABLES

LIST OF FIGURES

FIGURES

LIST OF ABBREVIATIONS

RRT	Rapidly exploring Random Tree
U-RRT*	Upgraded Rapidly exploring Random Tree Star
Scen1	Scenario 1
Scen2	Scenario 2

Chapter 1

Introduction

In this fast-evolving era, the demand for advanced technologies continues to grow. These technologies facilitate human life by providing assistance or even replacing human effort, regardless of the application field or nature of the task. One domain where this technological advancement is particularly evident is medicine, which continuously seeks new visions to improve patient consultation, diagnosis, therapy, and treatment. The surgical sector, in particular, has experienced significant technological evolution, ranging from machines and robots fully operated by humans to the development of increasingly autonomous surgical systems.

Robotic surgery offers several advantages over traditional surgical methods, including reduced trauma, faster patient recovery, and enhanced precision and efficiency in task execution. As minimally invasive procedures gain wider adoption, the importance of meticulous preoperative preparation and offline path planning becomes increasingly evident. Rather than solely depending on real-time autonomous decision-making, the ability to strategically plan surgical trajectories and actions prior to the procedure is critical for ensuring accuracy and safety, especially in complex anatomical regions. One of the central challenges in robotic surgery is equipping the system with a carefully optimised plan that anticipates possible complications and variability. Robust offline planning not only improves surgical precision but also plays a role in mitigating risk associated with unexpected Intraoperative events, thereby enhancing overall surgical outcomes.

To address these challenges, ongoing research explores various strategies, including strategy optimization, obstacle avoidance, and an advanced control system. For example, the study presented by (Cursi & Kormushev, 2021) introduces an offline, preoperative system designed to identify the optimal insertion point for surgical tools by integrating the remote centre of motion (RCM) constraint. While this approach enhances safety and accuracy, it is hindered by computational complexity and deployment challenges, primarily due to the iterative optimisation required over a discretised search space. Another promising development involves the use of artificial intelligence (AI) preoperative planning, particularly Deep Neural Network (DNN)

models combined with 3D printing technology to enhance surgical precision and efficiency (J. Wang et al., 2024). However, this technique still faces notable limitations, such as instability and precision issues with guide frames including screw deviation from plan trajectories. Furthermore, the rigidity of the frame may lead to systematic errors but affect multiple placements simultaneously. A third noteworthy contribution is the final element modelling (FEM)-based framework for optimising preoperative planning in thermal ablation of brain tumours, as proposed in (Zhao, Jiang, Bales, Wang, & Fischer, 2024). While this approach offers improved planning accuracy, it also raises concerns about computation and time constraints due to the intensive simulation requirements of FEM based analysis.

1.1 Statement of the Problem

In surgery, executing precise tasks like incision or suturing with a surgical robotic arm necessitates high levels of accuracy, smooth trajectory planning, and operational safety to minimise damage to surrounding tissues. The robotic system must be capable of following a predefined path while adapting to patient-specific constraints such as anatomical geometry, insertion point, and the proximity of critical structures, including blood vessels and vital organs. However, conventional path planning algorithms, particularly Rapidly exploring Random Trees (RRT) and their variants, often produce suboptimal trajectories characterised by limited smoothness and inefficient space exploration. This highlights the pressing need for more advanced path planning methods that can achieve a balance between trajectory smoothness, obstacle avoidance, execution time and computational efficiency in complex surgical scenarios.

1.2 Purpose of the Study

This study intends to develop and simulate an upgraded offline RRT* path planning algorithm tailored for surgical robotic arms, with the objective of generating precise, smooth, and continuous trajectories suitable for surgical interventions while effectively navigating around obstacles within the operational workspace. To validate

the effectiveness of the proposed algorithm, the following sub-hypothesis are formulated:

H1: Goal-biased sampling will reduce the average time required to find a valid path compared to the standard RRT algorithm.

H2: Implementing a clearance mechanism will maintain a safe distance from obstacles, thereby reducing the likelihood of collision and enhancing the reliability of the path

H3: Applying 4th-degree B-spline interpolation with a rotation matrix will significantly improve the smoothness of the path without increasing total computational time beyond 2 seconds.

H4: The upgraded algorithm will consistently outperform RRT and RRT connect in terms of both efficiency and reliability in a complex, obstacle-rich environment.

The structure of this document is organised as follows: Chapter 2 provides an overview of various path planning algorithms, with a focused analysis of RRT, RRT connect, RRT star and their associated limitations. Chapter 3 outlines the research methodology and details the procedural steps undertaken in the course of this study. Chapter 4 presents the results obtained, along with relevant evaluations and performance assessments. Finally, Chapter 5 discusses the key findings, draws conclusions, and proposes potential directions for future work.

Chapter 2

Literature Review

The literature review in this study will explore the state-of-the-art algorithms employed in offline path planning techniques for robot-assisted surgery, with a particular focus on methods that enable precise, reliable motion planning in complex anatomical environments. It will also explore the RRT algorithm and its variants. While considerable research has been directed towards real-time adaptive path planning, offline strategies remain essential for preoperative planning, offering the advantage of generating optimised, well-defined trajectories without the computational constraints of intraoperative adjustment. This preoperative approach contributes significantly to surgical precision by enabling efficient and constraint-aware movement planning ahead of execution.

Several notable studies have advanced this domain. For instance, the work in (Tzanetis et al., 2023) leveraged preoperative computed tomography (CT) imaging and statistical shape models to develop patient-specific musculoskeletal representations, aiding in preoperative trajectory planning. A quadratic optimization function was used to minimise deviations in kinematics and ligament strain from the Pre-disease state of the knee. Despite its precision, the computational time of approximately 32 hours poses limitations for use in time-sensitive clinical settings. Building on this, the study in(*2019 IEEE/RSJ International Conference on Intelligent Robots and Systems (IROS)*, 2019) proposed a hybrid approach combining the Bidirectional Continuous Tree Search (BCTS) algorithm with Bayesian optimization (BO) and a Radial Basis Function Neural Network (RBFNN) to enhance the smoothness and efficiency of offline preoperative path planning.

2.1 Overview of Path-Planning Algorithms

To start, we can consider (Y. Zhang, Ju, Zhang, & Qi, 2022), that makes use of the Rapidly Exploring Random Trees star (RRT*) algorithm and incorporates motion constraints of flexible needles to ensure smoother and more feasible paths. Nonetheless, this study underlines a poor optimisation of the trade-off between

accuracy and safety. (Ryan Luna, 2013) introduces a Meta-algorithm that combines traditional sampling-based motion planning with post-processing optimisation techniques to achieve continuous improvement of the planned trajectory. (H. Zhang, Zhu, Shen, & Song, 2023) proposes the method of Implicit Neural Field (INF) to guide teleoperated robotic surgery, but has a limited applicability to articulated or steerable surgical tools. (Hang Su, Jamal Sheiban, Qi, Salih Ovur, & Alfayad, 2024) employs Virtual reality (VR) for a robot-assisted surgical training system for robot-assisted minimally invasive surgery (RA-MIS). The system uses wearable sensorised gloves and Myo controllers for the manipulation of robotic surgical tools. High dexterity and controlled manoeuvrability are possible by utilising the system of concentric tube robot (CTR) that uses a fluorescent imaging probe to enhance precision in soft tissue imaging, helpful in the motion planning (Thamo et al., 2024). Then comes the introduction of an indirect trajectory planning method based on a three-stage evolutionary algorithm to optimise motion and planning, an application that ensures collision-free motion planning while minimising execution time(Abu-Dakka, Rubio, Valero, & Mata, 2013). Still, the cubic splines on which the method relies for trajectory generation may not always ensure jerk-minimised smooth motion. (Hao et al., 2022) Instead applies an improved Artificial Potential Field (APF)-based path planning algorithm that offers safety and accuracy in robot-assisted spine surgery. The dynamic gravitational constant and piecewise function are introduced to address common issues in traditional APF, such as local minima and target unreachability near obstacles. Despite the amazing benefits of this application, the burden of computational cost due to the combined APF and PDNN requires continuous real-time computation. Also, processing time is considerably increased because of obstacle avoidance constraints and the joint limit checks. (Tavares, Martins, & Tsuzuki, 2011) suggest the implementation of Simulated annealing (SA) with the adaptive neighbourhood approach, which is designed to handle cost functions with nonlinearities, discontinuities and stochastic elements, making it suitable for robot path planning. However, the study uses three different path representations, but it does not evaluate higher-order splines that could produce smoother and more energy-efficient paths. To add, (Santos, Rade, & da Fonseca, 2022) put forward an off-line path planning approach that combines several optimisation criteria together with machine learning. This approach, however, has limited scalability as it considers only a 3-DOF space

manipulator. (Bernardes, Adorno, Poignet, & Borges, 2013) introduces an Arc-RRT that uses input sampling instead of point sampling, along with explicit geometric constraints, that together ensure feasible trajectories and increase efficiency. Dual Reward and Policy Offline Inverse Distillation (DROID), an offline imitation learning from heterogeneous demonstrations used by (Jayanthi et al., n.d.) is a method used for Mars Rover Path Planning (MPP). A safe and precise glioma resection was performed thanks to the implementation of a modified RRT algorithm for a safe and feasible path using a cost function (Manrique-Cordoba, Martorell, Romero-Ante, & Sabater-Navarro, 2024). This application assumes that the preoperative MRI/DWI data remains unchanged during surgery, while brain shifts, deformations due to swelling and tissue movement may occur intraoperatively. From (Weber, Gambao, & Brunete, 2023) it is clear that there are numerous applications for offline path planning, like slicing, sectioning or differential geometry-based, which can all be implemented and tested using various simulation tools like ROS or RobokDK. The implementation of innovative Path Planning for Coreless Filament Winding (CFW) (Hügle, Genc, Dittmann, & Middendorf, 2022) presents a parameter-based method that includes the analytical Tool Center Point (TCP) trajectory generation, later on validated using Finite Element Method (FEM) simulations. Only, there is a shortage of time and energy optimization consideration, and it requires manual adjustments for collision avoidance. (Sundaram, Budjakoski, Klodmann, & Roa, 2022) suggest a Robot-Assisted Surgical System Capability Maps (RASSCMAP) for the base pose optimisation. Nevertheless, the application does not address much consideration to the two-collision avoidance. (Chakraborty et al., 2022) puts light on the varieties of algorithms for path planning, depending on the understanding of every algorithm's strengths and weaknesses and the various areas of application of each algorithm. Another implementation of AI is the use of novel reinforcement learning-based path planning that proposes a heuristically accelerated deep Q-network (HADQN) to optimise path planning for steerable needle insertion in neurosurgery. This provides great advancements in neurosurgery but still lacks energy and speed optimisation that reduces the actuation force of the needle and ensures safety(G. Ji, Gao, Zhang, Cao, & Sun, 2023). In the comparative study presented by (Kisinde, Hu, Hesselbacher, & Lieberman, 2021), the Mazor X-Align software provides 3D preoperative surgical planning. This software automates anatomical segmentation, accounts for a range of

motion limitations, and simulates spinal correction modification. (Delaney, 2024) drives through the evolution from 2D to advanced 3D software-based planning for preoperative planning that guides implant placement. Following is the application of Inverse Reinforcement Learning (IRL) for path planning during neurosurgery, and later compares this method to other path planning methods. The fact that the IRL model learns from a simulated brain environment may bring about overfitting as the real case scenarios may differ considerably(Segato et al., 2022). On the other hand, (Lin, Xie, Wang, & Wang, 2023) proposes a Deep Reinforcement learning (DRL)-based approach for preoperative planning of intra-operative ultrasound. It focuses on a 4-DOF cardiac ultrasound robot that addresses the challenge of optimal probe positioning. The approach leverages a double Deep Q-Network (DQN) for path planning but still fails to guarantee effective energy and time optimisation. (Hao Su et al., 2022) shows the usefulness and applicability of MRI in path planning during surgeries. (Monfaredi et al., 2024) Dives through the different pre-operative path planning for minimally invasive surgery based on different parameters like surgical tools, type of surgery, and anatomical considerations. A further implementation of path planning is in gynaecology for procedures like hysterectomy, myomectomy and endometriosis surgery (Alkatout, O'Sullivan, Peters, & Maass, 2024). The method uses a modular platform designed to integrate the robotic and laparoscopic techniques. In an environment with multiple obstacles, the study (Jiang, Liu, Cui, & Jiang, 2022) proposes the combined application of Improved RRT and Artificial Potential Field (APF). The RRT algorithm addresses path planning in complex, multi-obstacle environments, while APF optimises the path and ensures efficiency and collision avoidance. This application, however, is not time-effective. (Zhong, Wang, & Cheng, 2022) jointly implement Deep Reinforcement Learning (DRL) and Inverse Kinematics (IK) by integrating Deep Deterministic Policy Gradient (DDPG) with IK and introducing a gain module to balance exploration and exploitation. This ensures smooth and collision-free trajectories but does not have energy efficiency considerations. For a collision-free path, (Y. H. Yu & Zhang, 2022) developed an optimized slice-based Heuristic Fast Marching Tree (SH-FMT) algorithm which enables a better node placement and is highly efficient when compared to RRT, RRT* and FMT**. However, there is a lack of hardware consideration. As an attempt to resolve the issue of slow convergence speed and low search efficiency, (Yi, Yuan, Sun,

& Bai, 2022)study employs an improved P_RRT algorithm for path planning that involves a dual-expansion strategy for new nodes, a cost function to optimise nearest neighbour selection and redundant node deletion for path smoothing. (Pan, Zhang, Xia, Xiong, & Shao, 2022), in order to enhance local minima generally present during the application of APF for path planning, introduces an improved version of APF (IAPF). (C. Cheng, Sha, He, & Li, 2021) sweeps through various path planning applications like A*, genetic algorithm (GA), Particle swarm optimisation (PSO), Ant colony optimisation (ACO) and differential Evolution (DE) to name just a. They analyse them under different criteria and compare their results to understand their strengths and weaknesses. (H. Shen, Xie, Tang, & Zhou, 2023) Proposes a money pool ability-based optimal rapidly exploring random tree star (RRT*) path planning strategy for industrial robot manipulators, using path length and manipulability both as constraints and evaluation metrics. They also implement adaptive step size in RRT to improve search efficiency. (Yang Wen, Haiying, & Zhisheng, 2021) designed an improved RRT star (RRT*) that introduces a target probability offset, ensuring faster conversions by biasing the random sampling towards the goal and also a variable step size control, which helps in escaping local minima, making the algorithm more efficient. ('Robot Arm Path Planning Based on Improved RRT', n.d.) also present an improved RRT algorithm for robot arm path planning, focusing on target probability biasing invariable step size control to ensure frequent sampling towards the goal and prevent the algorithm from getting trapped in local minima. Another improved RRT star algorithm for a 6-axis manipulator path planning in an obstacle-field environment is proposed by (Liu & Cao, 2022) with two key improvements in enhanced path pruning and reduction of the global sampling space. (Zhuang, Li, & Ding, 2023) present an obstacle avoidance path planning method that instead implements an artificial potential field (APF) whose local minimum issue is corrected by improved rapidly exploring random tree star (RRT*) and A* algorithm. (Dai, Zhang, & Deng, 2024) jointly implement artificial potential field (APF), goal-biased bi-directional RRT* and direct connection strategy. (Demir, 2021) combines the application of Genetic Algorithms (GA), Particle Swarm Optimisation (PSO) and Artificial Potential Field, which are all heuristic methods. Another advancement of the RRT* algorithm is presented by (H. Ji, Xie, Wang, & Yang, 2023) that employs an Ellipsoidal-Shape RRT* algorithm with which the contributions are: incorporating angle constraints, using ellipsoidal connection

strategy, slow-speed informed sampling and path smoothing using polynomial interpolation. (R. Wang, Xie, Chen, & Li, 2023) formulates a novel method of third-order Time-Optimal Time Scaling (TOTS), divided into four stages; the first two compute the second-order optimal velocity profile while the third and fourth stages eliminate jerk constraint violation. (Shao et al., 2021; Shi, Wang, Zhao, & Tian, 2022) integrates a Goal-biased RRT algorithm and bi-directional path smoothing. AN investigation study conducted by (Duan & Zhang, 2022) aims to evaluate various polynomial-based trajectory planning methods using the Lagrangian-Euler dynamics model to calculate energy consumption. (Wei, Zheng, & Gu, 2021) presents a specialised, rapidly exploring random tree (Sp-RRT) approach for Follow-the-leader (FTL) motion planning of hyper redundant manipulators in confined environments. (Yalun Wen & Pagilla, 2023) proposes for path planning implementation, a trajectory optimisation using the orthogonal collocation method in which states are represented with Legendre polynomials in Barycentric form, and the problem is converted into a discrete nonlinear programming (NLP) formulation. And a collision avoidance method. (Long, Li, Zhou, & Chen, 2023) enhances RRT* with a dynamic A* cost function sampling method, a path pruning strategy, Dynamic region path repair and regrowth, and Quintic NURS and Particle Swarm Optimisation (PSO). (Song et al., 2021) suggest an adaptive robust control method using a Radial Basis Function (RBF) Neural Network to improve trajectory and Quintic polynomial to smooth the path. (Massaro, Lovato, Bottin, & Rosati, 2023) introduces a nonlinear optimal control approach (NLP) that employs a pseudo-spectral collocation method for numerical solutions and incorporates actuator constraints. Another implementation of RRT is proposed by (Tian et al., 2021), in which redundant nodes are reduced using Parent Point Priority Determination (PPD). (Yuan, Yi, Sun, & Bai, 2021) combiene the strengths of Improved Artificial Potential Field (I-APF), which is heuristic-based and Improved Rapidly exploring Random Trees (I-RRT) which uses a triangular nearest-neighbor node selection strategy and adaptive step sizes. The heuristic path planning method for a tomato-bunch harvesting robot that integrates a 3D-Convolutional Neural Network (3D-CNN) based position Posture Map (PPM) with rapidly exploring random tree (RRT) algorithm (Q. Zhang, Liu, & Li, 2023). A simultaneous search for both the optimal path and the optimal motion time using a cubic uniform B-spline interpolation and an improved genetic algorithm (X. Yu, Dong, & Yin, 2022). (Gao, Yuan, Sun, &

Xu, 2023) execute a novel BP-RRT* using a Backpropagation (BP) Neural Network to enhance RRT* in a 3D environment with dense obstacles. (X. Cheng et al., 2023) proposed improvements to RRT-Connect with; adaptive step size strategy, Fixed sampling function instead of random sampling and Four-tree seach method. (Fairchild, Srivastava, & Tan, 2021) addresses computational challenges associated with traditional obstacle modelling and proposes an improved geometric approach using parametric equations instead of point-based representations. ('Towards Comparison and Real Time Implementation of Path Planning Methods for 2R Planar Manipulator with Obstacles Avoidance. ', n.d.) employs rational Bezier and NURBS algorithms for path planning to ensure path continuity and smoothness. (Q. Cheng, Zhang, Liu, Zhang, & Hao, 2021) formulates a hybrid path planning algorithm that employs a Gaussian Mixture Model (GMM), Gaussian Mixture Regression (GMR) and a Modified Probabilistic Roadmap (MPRM). (Rajendran, Thakar, Bhatt, Kabir, & Gupta, 2021) uses a bidirectional tree search. Initially, a previously created tree search is expanded, then secondly includes novel scheduling logic and tactics that reduce both the planning time and the failure rate. Lastly, an approach for inter-tree connections that adjusts to collision data collected over time. (J. Xu & Wang, 2022) presents an improved motion planning algorithm called SDPS-RRTConnect, which enhances the standard RRTconnect method by improving it based on a Sparse Dead Point Saved (SDPS) strategy. (LIU Yaqiu, 2021) Employ an Improved RRT that integrates an extension-point selection strategy, an adaptive step-size strategy, a local minimum avoidance mechanism and the Dijkstra algorithm for optimisation of the planned path. (Y. Wang et al., 2022) improves the RRT algorithm with an intermediate bias point strategy and path shortening techniques.

2.2 Overview of RRT-Based Algorithms

2.2.1 RRT algorithm. This probabilistic sampling-based approach incrementally expands a tree structure. By randomly selecting points within the state space, the algorithm efficiently explores unoccupied regions, guiding the search towards a feasible path from the initial point to the target destination(Y. Shen, Liu, & Luo, 2021)

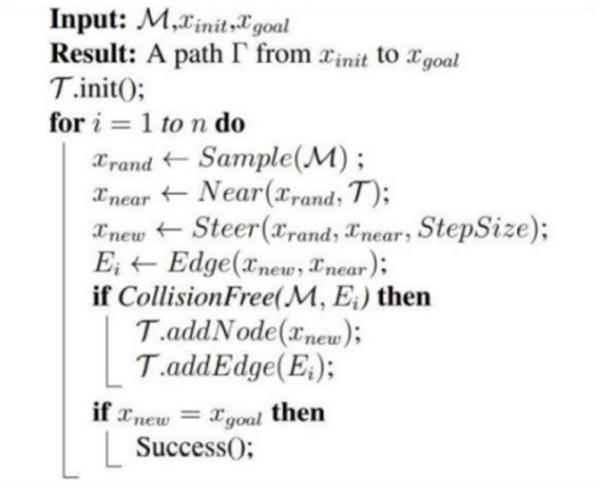

Figure 1. Pseudocode representation of RRT algorithm(Yao, 2024). x denotes various parameters according to the subscript. M represent the configuration space, T represent the tree structure, and E is a representation of the edge in the tree. The ".addNode" and ".addEdge" are functions associated with T.

The rapidly exploring Random Tree (RRT) algorithm builds a tree through random sampling within the search space. The tree originates from a defined initial node denoted Node _init and expands iteratively to find the path toward the goal state, goal. As iteration progresses, a random node (Node_rand) is selected from the configuration space (2D, 3D). If this randomly chosen node lies in a collision-free region, the algorithm identifies the nearest node, Node_nearest, within the tree using a predefined metric. If the Node_rand is reachable from Node_nearest within a specified step size, the tree extends by connecting the two nodes. Otherwise, a new node, Node_new, is generated using a steering function, and the tree is expanded by linking Node_new and Node_nearest. A Boolean collision check ensures that the connection between Node_new and Node_nearest is free of obstacles. Another Boolean checks if the goal is reached, and the algorithm stops if that's the case(Yao, 2024).

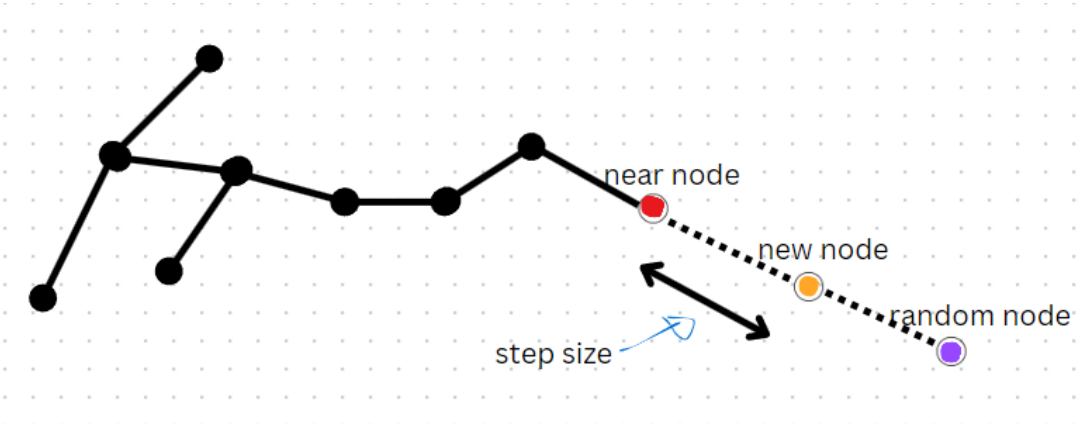

Figure 2. Process of RRT algorithm tree expansion. This illustration shows a typical step in the RRT algorithm's tree expansion. The purple point is the random point generated at the beginning of the loop, and according to which, a nearnode is selected (in red). According to the step size, a newnode (orange) is added.

2.2.2 RRT connect algorithm. The RRT-Connect uses two randomly growing trees within the free space. One tree originates from the starting point, Qinit, while the other begins at the target point, Qgoal. These trees expand bidirectionally, exploring free space and alternately generating new nodes, denoted Qnew, and a check is performed to determine if the Euclidean distance between Qnew and the nearest node in the other tree is less than a predefined step length ε. If the distance is within this threshold and there are no obstacles along the connection, the two nodes are linked, effectively merging the two trees into a single structure and forming a complete path from the start to the goal (Yang, Li, Liu, Yu, & Li, 2021).

Begin *RRT-Connect* **Procedure**
$T_a \leftarrow$ **Insert** Root Node<q_{start}> to T_a
$T_b \leftarrow$ **Insert** Root Node<q_{goal}> to T_b
While $1 \leftarrow n$ to N **do**
  Generate n-th Random Sample
  $q_{rand} \leftarrow$ Position of n-th Random Sample
  If Not *Extend*(T_a, T_b, $q_{newB} \leftarrow$ ***Null***, q_{rand}, λ, C) **then**
    If *Connect*($P_{reach} \leftarrow$ ***Null*** Path, T_a, T_b, q_{newB}, λ) **then**
      $d_{reach} \leftarrow$ Distance of P_{reach}
      If $d_{shorter} = 0$ **or** $d_{shorter} > d_{reach}$ **then**
        $R \leftarrow P_{reach}$
        $d_{shorter} \leftarrow d_{reach}$
  Swap(T_a, T_b)
End *RRT-Connect* **Procedure**

Figure 3. Pseudocode for the RRT-Connect algorithm(Kang, Lim, Choi, Jang, & Jung, 2021). Depending on its subscript, p denotes various parameters. λ is similar to ε and denotes the stepsize. dreach is the distance associated with Preach (checking parameter for goal reached), and dshorter tracks the shortest path found.

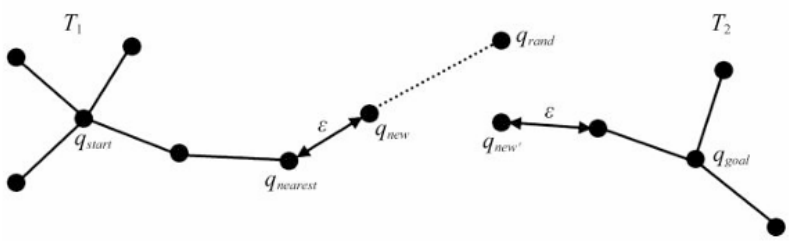

Figure 4. RRT-Connect working principle (Chen, Fu, Zhang, Fu, & Shen, 2022). q refers to different parameters represented by the subscript attached to it. ε is the step size used for tree extension, while the dashed line shows the final connection. T denotes the tree, which in this case are two (T1 and T2).

2.2.3 RRT star algorithm (RRT*). RRT* takes over the properties of RRT and works alike but introduces an optimization step that evaluates whether a newly added node can be reconnected to a different parent node for a lower overall path cost. If a more efficient parent node is found, the tree is restructured in a process known as rewiring, which relies on the neighbourhood radius, r. The radius defines a search region around the new node to find a lower cost parent. The neighbourhood is ideally set to 2-3 times the step size for effective rewiring(T. Xu, 2024). γ is the user-defined constant, n is the number of nodes, and d represent the dimension of the configuration

$$r = \gamma \left(\frac{\log(n)}{n}\right)^{\frac{1}{d}} \quad 1$$

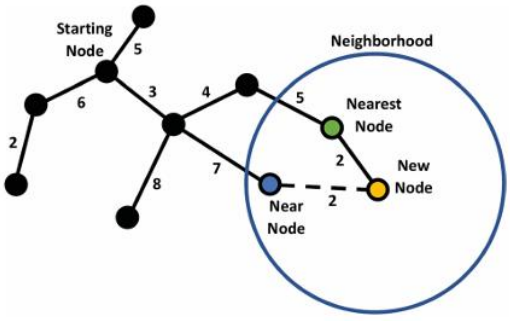

Figure 5. RRT* parent cost check and neighbourhood radius representation (Mohammed, Romdhane, & Jaradat, 2021). This figure illustrates how the RRT* evaluates parent node costs within a defined neighbourhood. The neighbourhood is the rewiring search area selected by the user and is larger than the stepsize.

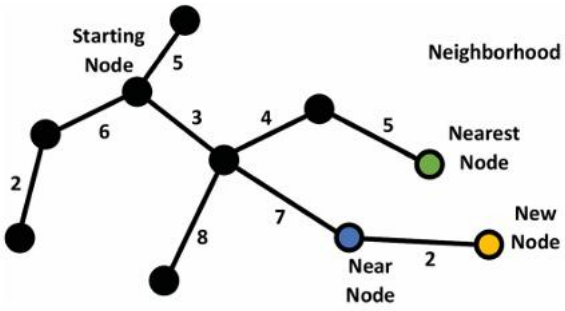

Figure 6. Representation of RRT* node reconnection to lower cost parent(Mohammed et al., 2021). After a better parent is found, the link is deleted with the previous one and created with the new parent.

$T \leftarrow$ InitializeTree();
$T \leftarrow$ InsertNode($\emptyset$, z_{init}, T);
for i=0 to i=N ***do***
$z_{rand} \leftarrow$ Sample(i);
$z_{nearest} \leftarrow$ Nearest(T, z_{rand});
(z_{new}, U_{new}) $\leftarrow$ Steer ($z_{nearest}$, z_{rand});
if Obstaclefree(z_{new}) ***then***
    $z_{near} \leftarrow$ Near(T, z_{new}, $|V|$);
    $z_{min} \leftarrow$ Chooseparent (z_{near}, $z_{nearest}$, z_{new});
    $T \leftarrow$ InsertNode(z_{min}, z_{new}, T);
    $T \leftarrow$ Rewire (T, z_{near}, z_{min}, z_{new});
return T

Figure 7. Pseudocode representation of RRT* algorithm(Noreen, Khan, & Habib, 2016). Here, z represents different points and node parameters depending on the subscript associated with it. |V| represent the number of nodes in the tree. T is the tree parameter. Unew is the control input.

Chapter 3

Methodology

This chapter outlines the methodological framework employed to evaluate and compare existing path-planning algorithms with the upgraded version of RRT* proposed by this study in a structured and consistent manner.

3.1 Environment Setup

All three algorithms (RRT, RRT-Connect, Upgraded-RRT) were executed under the same conditions to ensure fair evaluation. In a main m-file, all the algorithms are called to run starting from RRT, through RRT connected to the Upgraded RRT star. For each algorithm, a 3D occupancy grid map was developed, to which obstacles were added. It served as the simulation environment. The code in the main m-file ran all the algorithms called for a given number of trials (20 in this study), and for each set of 20 trials, initialized parameters like step size and max number of iterations were kept constant for effective performance assessment purposes. The parameters were the same for each algorithm except parameters that are specific to an algorithm like the binding distance for RRT connect. There were the same predefined start and goal positions, and the environment was populated with two distinct obstacle densities.

- Low Obstacle Density (Scen1). A scenario with relatively few obstacles. This represents surgical regions like the skin.
- High Obstacle Density (Scen2). A scenario with numerous obstacles creates a clustered environment. This may represent a surgical region like in vivo surgery at the level of the belly or the chest, where organs other than the organ on which surgery is performed are considered obstacles.

For each scenario, a set of 20 trials each was run. This unified approach ensures consistent comparisons across methods, isolating the effect of the planning algorithm itself. We recorded the outcome of each run for later analysis, focusing on key performances described subsequently.

3.2 Algorithms Implemented

The implementation runs the sampling-based path planning algorithms RRT, RRT connected and the upgraded RRT* algorithm proposed by this study in the MATLAB platform as shown in Figure 8. Their performance was evaluated based on finding path efficiency, path length, computational time and path smoothness.

The Upgraded RRT* implements a Goal Bias Sampling Strategy with a bias probability of 0.2 (20%), used to increase the likelihood of sampling towards the goal, leading to a faster convergence. Given that surgery is carried in sensitive environment, it is not sufficient not to touch the obstacle (which in anatomical environment are other organs) but also to stay at a distance from the obstacle to anticipate any abrupt movement of an obstacle, this upgraded version incorporates a Clearance-based Collision Avoidance in which a minimum clearance threshold is set to ensure that the new node does not collide with the obstacle and is at a certain distance from it. For this implementation, each obstacle is considered a 3D sphere and the node a 3D point. The code calculates the Euclidean distance (Equation 2) between the new node and the obstacle and compares the distance to the radius r of the obstacle plus the minimum clearance C. Also, a smoothing section, which uses a 4th-degree B-spline interpolation and a rotation matrix (illustrated in Equation 3 - 5), is added in the algorithm to improve the quality of the path and its feasibility. The Algorithm workflow can be seen in Figure 9.

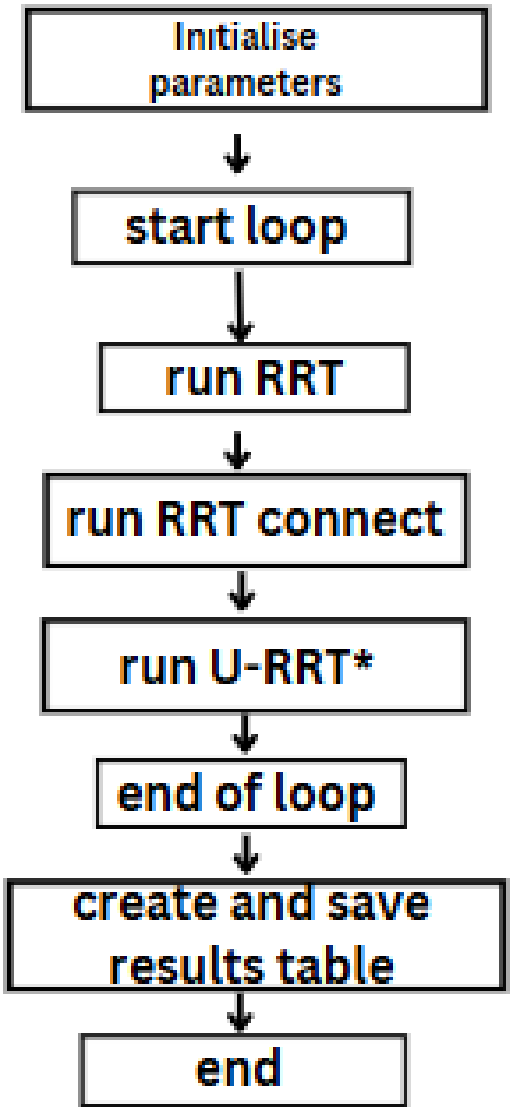

Figure 8. Workflow of the main Matlab script (m-file). This flowchart outlines the execution process of the primary Matlab script used to evaluate the performance of RRT, RRT connect, and U-RRT* algorithms. After initializing parameters, the script iterates through a specified number of trials (numTrial), running each path-planning algorithm in sequence. Upon completion of all trials, the script generates and saves a result table for further analysis.

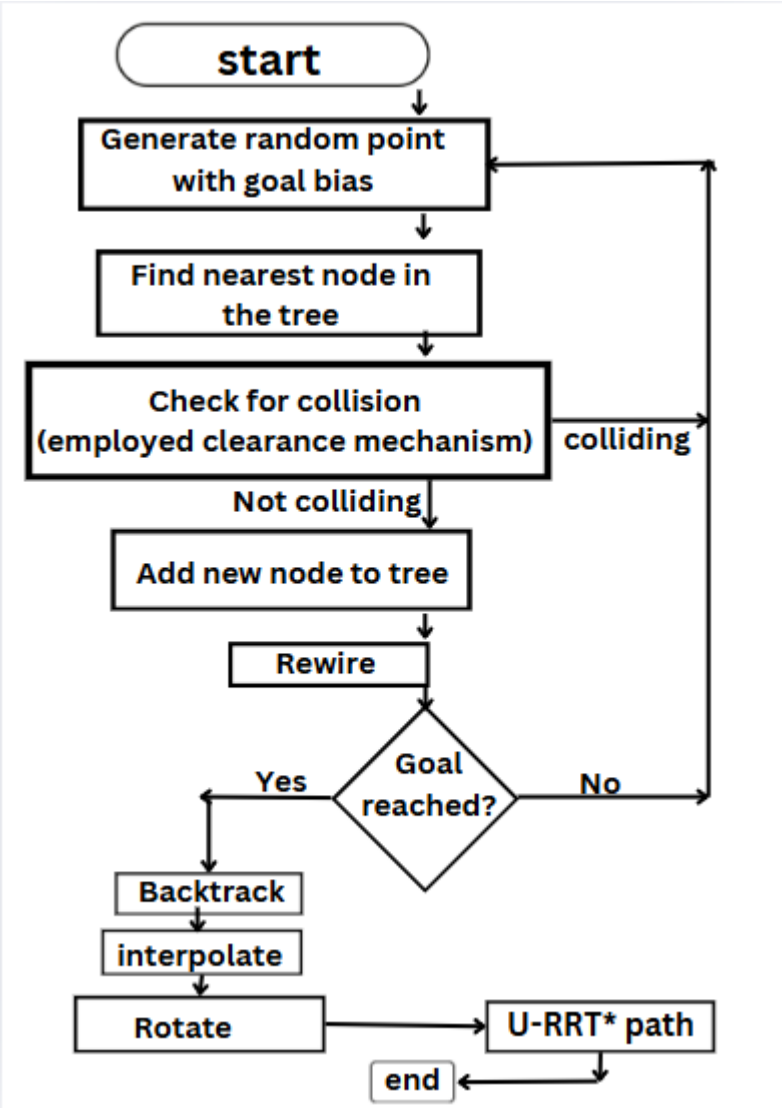

Figure 9. U-RRT* algorithm workflow. This diagram illustrates the complete path-planning process of the proposed U-RRT* method. The algorithm begins with random point generation influenced by a goal bias, finds the nearest node, performs collision checks using a clearance mechanism, and adds the new node to the tree. If necessary, it rewires and checks whether the goal is reached. If the goal is reached, the algorithm proceeds to backtrack and apply B-spline interpolation and a rotation matrix to generate a smooth and feasible path. Otherwise, the process repeats until a valid path is found.

In the following equation, d_i is the distance between the newNode and the centre of the i-th obstacle, $\vec{p}$ is the 3D coordinate of the newNode, $\overrightarrow{o_i}$ is the 3D coordinate of

the i-th obstacle centre, r_i is the radius of the i-th obstacle, and C is the minimum clearance.

$$distance\ (d_i) = \|\vec{p} - \vec{o_i}\| = \sqrt{(x - x_0)^2 + (y - y_0)^2 + (z - z_0)^2} \quad 2$$

If $\|\vec{p} - \vec{o_i}\| < r_i$ + C, then it's too close or in contact with the obstacle and the node is returned as colliding, thus not added to the tree.

The 4th-degree B-spline interpolation constructs a new set of points using Equation 3, where c(t) is the interpolation curve, and $N_{i,4}$ are the B-spline basis functions of degree 4, P_i are the control points (interpolation points). Each control point is typically a vector, $e.g,\ P_i = x_i, y_i, z_i$.

$$c(t) = \sum_{i=1}^{n} N_{i,4} \cdot P_i \quad 3$$

After generating the smooth interpolated path, the entire set of interpolated points is rotated such as to align the path with the desired orientation in the surgical environment. In Equation 4 below, $R_z(\theta)$ is the rotation matrix.

$$R_z(\theta) = \begin{bmatrix} \cos(\theta) & -\sin(\theta) & 0 \\ \sin(\theta) & \cos(\theta) & 0 \\ 0 & 0 & 1 \end{bmatrix} \quad 4$$

$$c'^{(t)} = R_z(\theta) \cdot c(t) \quad 5$$

This upgraded RRT* algorithm follows a structural approach to efficiently generate collision-free and smooth paths in a 3D environment in a remarkable amount of time. The workflow optimises fast node generation, collision avoidance and path smoothness while maintaining computational efficiency. Figures 9-14 show examples of how the different algorithms perform.

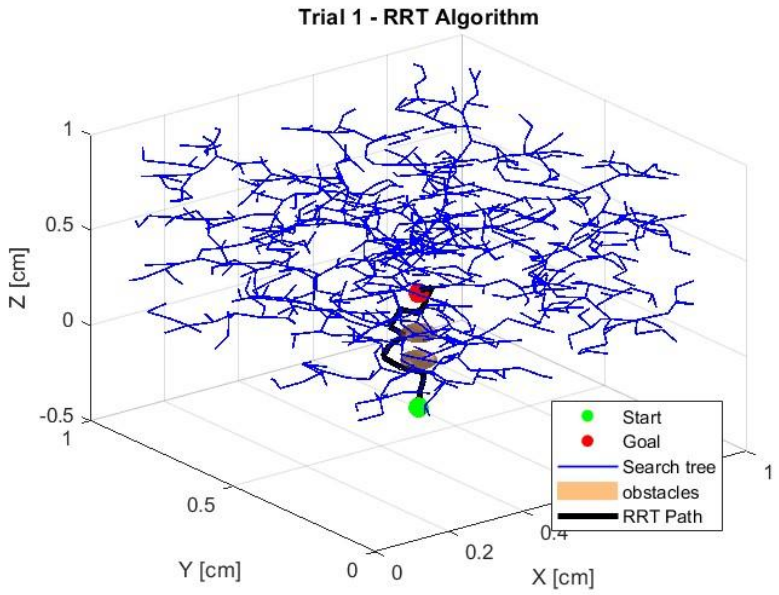

Figure 10. Visualization of RRT algorithm in scenario 1 (scen1). This plot illustrates the path planning using the RRT algorithm. The blue lines represent the search tree expansion, the orange spheres indicate obstacles, the green and red markers show the start and goal positions, respectively, and the bold black segments depict the final path found.

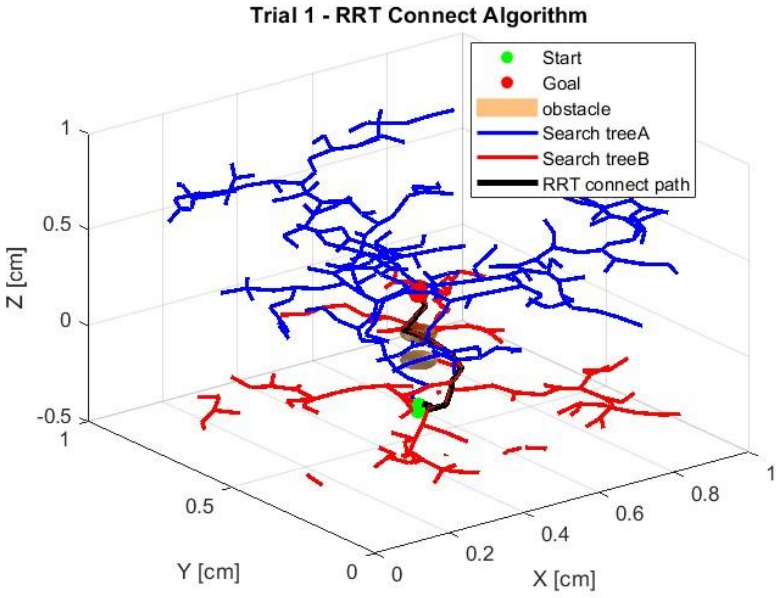

Figure 11. Visualization of RRT connect algorithm in scenario 1 (scen1). This figure illustrates the path planning process using the RRT-connect algorithm. Two rapidly growing search trees expand from the start (green) and goal (red) positions. The final connection path between the trees is indicated by the black line.

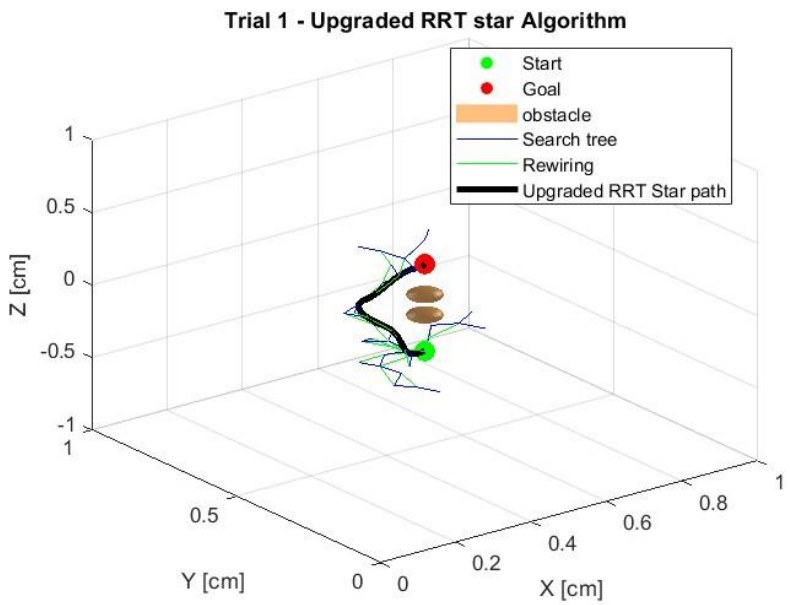

Figure 12. Visualization of U-RRT* algorithm in scenario 1 (scen1). The 3D plot presents the optimized path planning achieved with the proposed U-RRT* algorithm. The start and the goal positions are illustrated in green and red, respectively. The orange spheres represent the obstacles. The search tree is shown in blue, with the final smooth path marked in black. Rewiring steps are highlighted in green, indicating optimisation phases. The bold Black line indicates the path found.

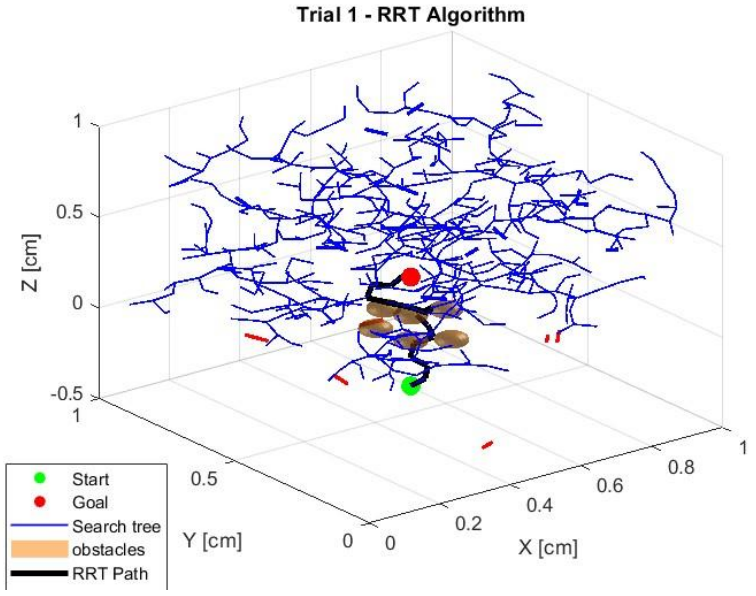

Figure 13. Visualization of RRT algorithm in scenario 2 (scen2). This plot illustrates the path planning using the RRT algorithm. The blue lines represent the search tree expansion, the orange spheres indicate obstacles, the green and red markers show the start and goal positions, respectively, and the bold black segments depict the final path found.

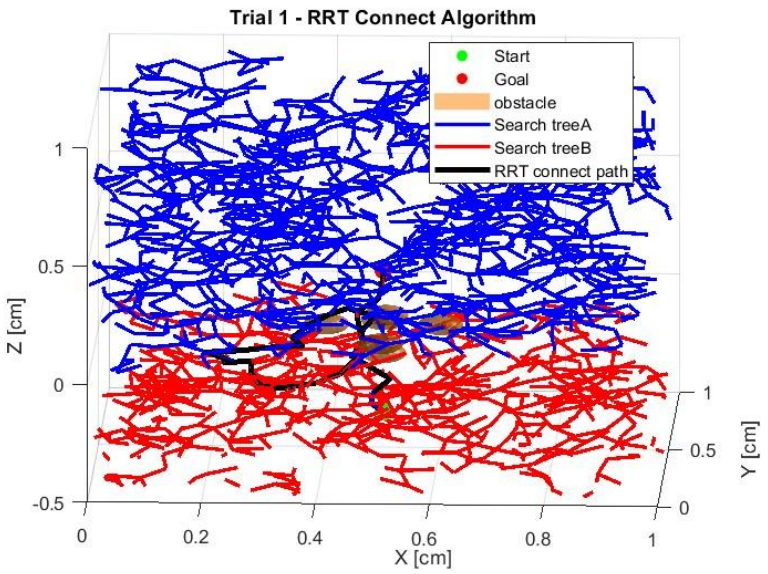

Figure 14. Visualization of RRT connect algorithm in scenario 2 (scen2). This figure illustrates the path planning process using the RRT-connect algorithm. Two rapidly-growing search trees expand from the start (green) and goal (red) positions, shown in blue and red, respectively. The final connection path between the trees is indicated by the black line.

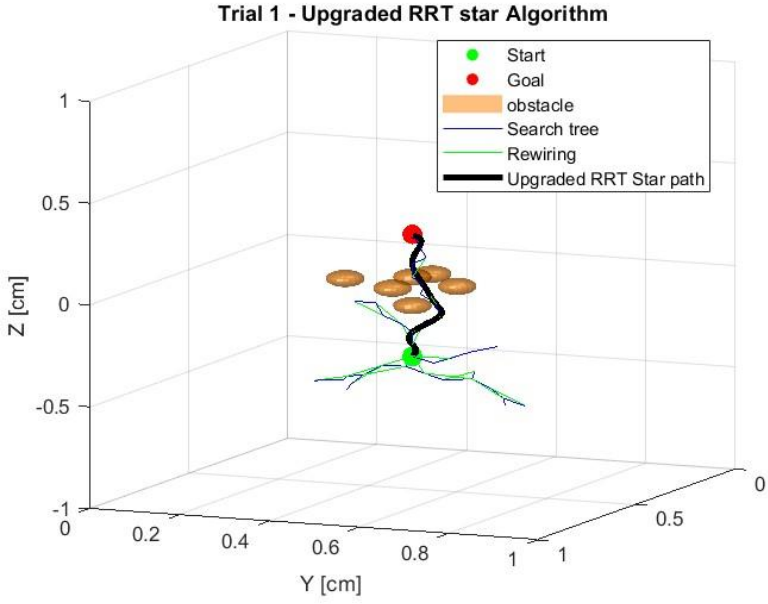

Figure 15. Visualization of upgraded RRT* in scenario 2 (scen2). This figure illustrates the path planning process using the RRT-connect algorithm. Two rapidly-growing search trees expand from the start (green) and goal (red) positions, shown in blue and red, respectively. The final connection path between the trees is indicated by the black line.

3.3 Performance Metrics

During each trial, the following performance metrics were recorded for each algorithm to evaluate and compare their performance:

- Execution Time. The time required for the algorithm to find a path from start to goal or determine that none is found within the limit of the maximum iteration. A shorter execution time indicates faster performance. It is measured using MATLAB's timing functions for each run and averaged over all trials per condition to compare efficiency across algorithms.

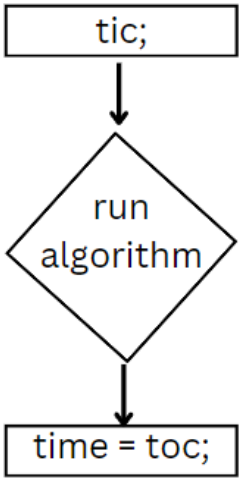

Figure 16. Workflow for recording execution time metric. The process begins by calling "tic" to start the timer, followed by the execution of the algorithm. Once the algorithm completes, "toc" is used to capture the elapsed time, which is stored for performance evaluation.

- Path smoothness. A quantitative measure of the quality of the path produced. In the context of this study, the smoothness of a path is assessed by considering the turning angles calculated at waypoints and the variance of the angles to classify the paths as either smooth, moderately smooth or stiff. The smooth path is indicated by low angles and low variance.
- Path Length. Which informs on the possibility of a smooth path and also reflects the feasibility of the path. It is measured by computing the Euclidean distance of the differential of the path.

- Search Success Rate. The percentage of trials in which the algorithm successfully finds a collision-free path to the goal. This metric captures the reliability of the planner under different circumstances. A 100% success rate indicates that the planner found a path in every trial, whereas lower rates mean occasional failure.

Together, these three metrics provide a comprehensive insight into performance: execution time reflects speed, path smoothness reflects path quality, and success rates reflect the effectiveness/robustness of the planning method.

Chapter 4

Findings

After running several sets of trials for code adjustments and adequate performance, two sets of trials were performed for two case scenarios: the few obstacles scenario (scen1) and the dense obstacle scenario (scen2). After each set was run, verifications were performed to ensure the metrics were appropriately recorded and the classification was well done. This section showcases all the results recorded and their analyses.

4.1 Test Scenarios and Results

The first scenario (scen1) reflects a low-density environment, while the second scenario (scen2) is about a high-density environment. In scen1, two obstacles are placed between the start and the goal points such that the algorithm is required to avoid these obstacles and still find a path to the goal. In scen2, four additional obstacles are placed at the four sides of the already present obstacles between the start and goal points. This increases the complexity of the search and the obstacle avoidance.

For the execution time metric and the path length, their means were calculated (Table 1) for every algorithm and then plotted (Figures 17-18). Later, an additional analysis was made using the one-way ANOVA statistical analysis method to effectively compare the RRT and RRT connect algorithms' results to those of U-RRT* separately. For the remaining parameters, Success rate, Path smoothness and Obstacle avoidance, percentages were calculated and reported in tables and then plotted using pie charts.

Table 1

Mean Values of Execution Time and Path Length for the Different Algorithms

	Execution Time/seconds			Path Length/centimetres		
Scenario	RRT	RRT connect	Upgraded RRT*	RRT	RRT connect	Upgraded RRT*
1	59.04	87.44	1.78	0.89	0.91	0.69
2	116.25	165.43	1.79	0.82	0.95	0.69

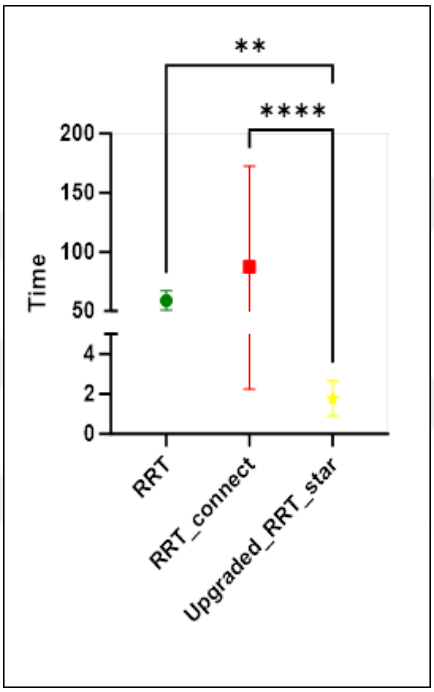

Figure 17. Execution time comparison for scenario 1 (scen1). This bar chart represents the execution time analysis of three path planning algorithms- RRT, RRT connect and U-RRT*- under the same environment (scen1). The vertical axis represents the execution time, with the statistical significance indicated by asterisks ($p < 0.05$ = *, $p < 0.01$ = **, $p < 0.001$ = ***, $p < 0.0001$ = ****). Variability across trials is represented by error bars.

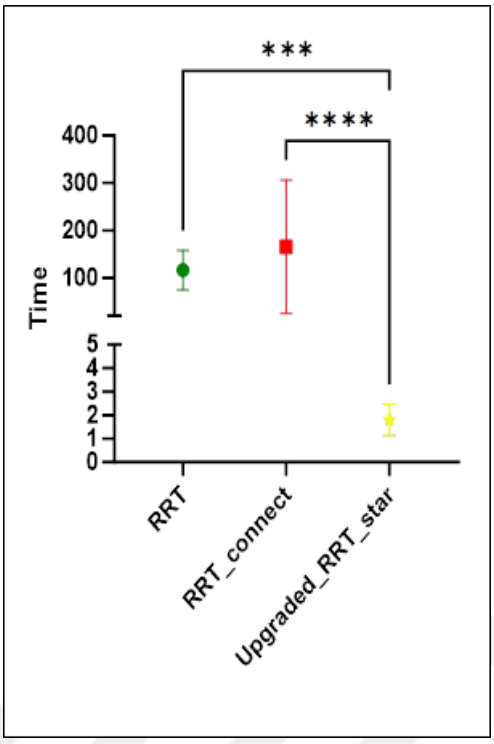

Figure 18. Execution time comparison for scenario 2 (scen2). This bar chart represents the execution time analysis of three path planning algorithms- RRT, RRT connect and U-RRT*- under the same environment (scen2). The vertical axis represents the execution time, with the statistical significance indicated by asterisks ($p < 0.05$ = *, $p < 0.01$ = **, $p < 0.001$ = ***, $p < 0.0001$ = ****). The error bars represent variability across trials.

The p-value differs according to the compared algorithms. In scen1, for the comparison between RRT and U-RRT*, the p-value is 0.0011 and for the comparison between RRT connect and U-RRT*, the p-value is 0.0001. Now, for the path length, the p-value related to the comparison between RRT and U-RRT* is 0.0779 and for the RRT connect and U-RRT* comparison, it is 0.0001. In scen2, for the execution time, the p-value is 0.0001 for both comparisons. Looking at the path length, the p-value is 0.0397 for the comparison between RRT and U-RRT*, while for the RRT connect and U-RRT* comparison, it is 0.0001.

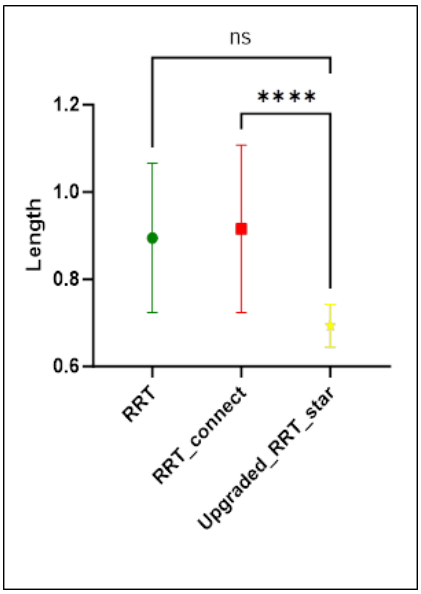

Figure 19. Path length comparison for scenario 1 (scen1). This bar chart shows the average path length generated by the RRT, RRT-connect and U-RRT* algorithms. The y-axis represents the length, and error bars represent standard deviation across trials. The statistical significance indicated by asterisks ($p < 0.05$ = *, $p < 0.01$ = **, $p < 0.001$ = ***, $p < 0.0001$ = ****) and ns (no significance) is returned where there is no significant difference.

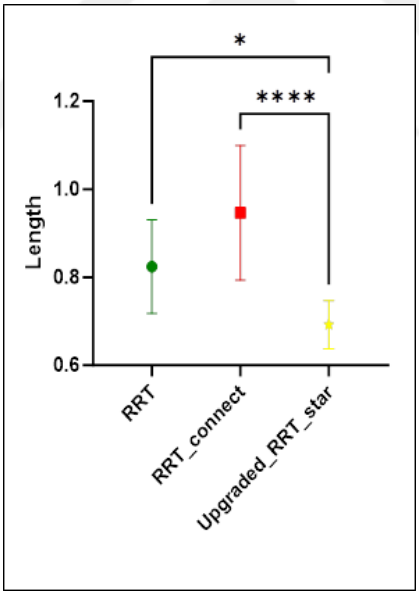

Figure 20. Path length comparison for scenario 2 (scen2). This bar chart shows the average path length generated by the RRT, RRT-connect and U-RRT* algorithms. The y-axis represents the length, and error bars represent the standard deviation across trials. The statistical significance indicated by asterisks ($p < 0.05$ = *, $p < 0.01$ = **, $p < 0.001$ = ***, $p < 0.0001$ = ****) and ns (no significance) is returned where there is no significant difference.

Table 2

Percentage Representation of the Success Rate of a Found Path

	Scenario 1			Scenario 2		
Classification	RRT	RRT connect	U-RRT*	RRT	RRT connect	U-RRT*
0	90	35	0	80	50	0
1	10	65	100	20	50	100

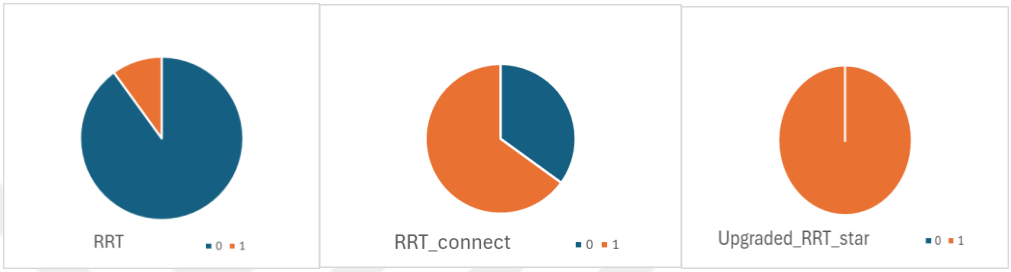

Figure 21. Success rate assessment for scenario 1 (scen1). This set of pie charts visually represents the success rate of path finding of RRT, RRT-connect and U-RRT* algorithms in scen1. The orange portion indicates successful trials (classification = 1), while the blue portion denotes failures (classification = 0).

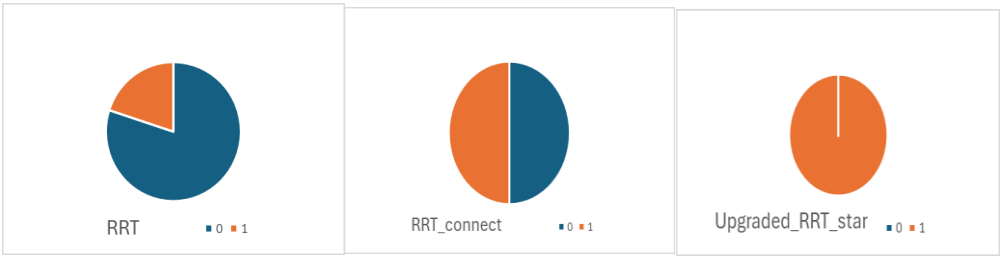

Figure 22. Success rate analysis for scenario 2 (scen2). This set of pie charts visually represents the success rate of path finding of RRT, RRT-connect and U-RRT* algorithms in scen1. The orange portion indicates successful trials (classification = 1), while the blue portion denotes failures (classification = 0).

Table 3

Percentage Representation of the Smoothness Metric

	Scenario 1			Scenario 2		
Classification	RRT	RRT connect	U-RRT*	RRT	RRT connect	U-RRT*
0	50	84.61	0	0	60	0
0.5	50	15.39	10	10	30	0
1	0	0	90	10	10	100

The percentage of the smoothness metric reflects the smoothness of the found paths only and does not consider cases where no path is found. 1 indicates a smooth path, 0.5 a moderately smooth and 0 indicates a stiff path.

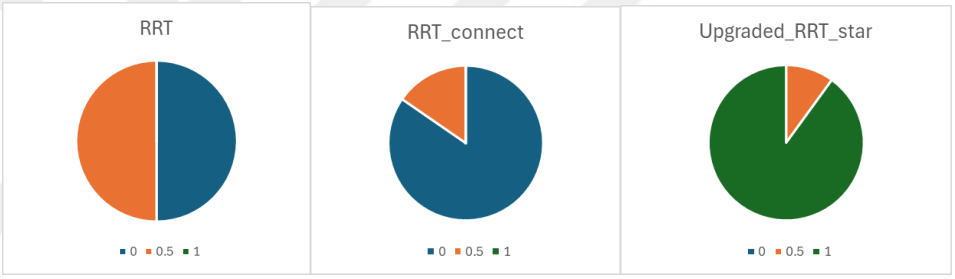

Figure 23. Path smoothness comparison for scenario 1 (scen1). This figure represents the smoothness classification results for the paths generated by RRT, RRT-connect and U-RRT* algorithms. The pie charts categorize smoothness into three levels: 0 = not smooth (in blue), 0.5 = moderately smooth (in orange) and 1 = smooth (in green).

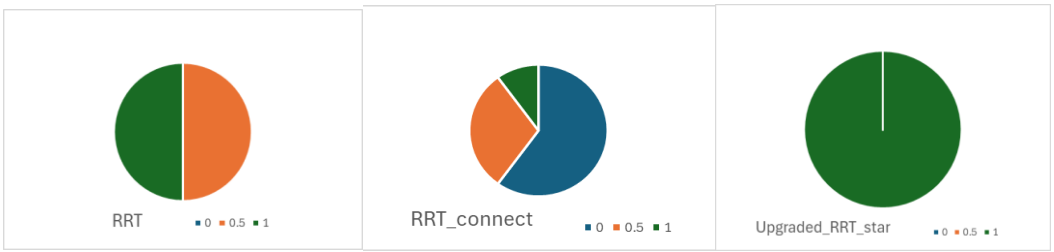

Figure 24. Path smoothness comparison for scenario 2 (scen 2). This figure represents the smoothness classification results for the paths generated by RRT, RRT-connect and U-RRT* algorithms. The pie charts categorise smoothness into three levels: 0 = not smooth (in blue), 0.5 = moderately smooth (in orange) and 1 = smooth (in green).

Table 4

Percentage Representation of Obstacle Avoidance

	Scenario 1			Scenario 2		
Classification	RRT	RRT connect	U-RRT*	RRT	RRT connect	U-RRT*
0	50	55.56	0	50	60	0
1	50	44.44	100	50	40	100

For the obstacle avoidance metric, the percentage reflects the effective obstacle avoidance of only planned paths, where 0 reflects failed avoidance and 1 reflects successful avoidance.

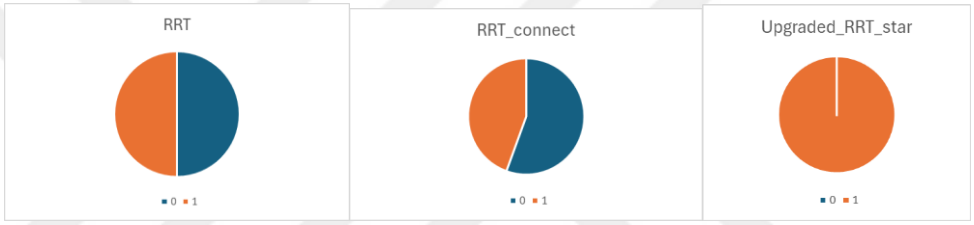

Figure 25. Obstacle avoidance assessment for scenario 1 (scen1). The orange section represents the successful avoidance (classification = 1), and the blue section represents the failed obstacle avoidance (classification = 0).

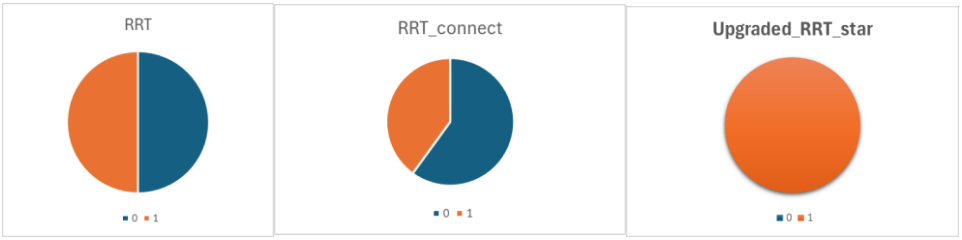

Figure 26. Obstacle avoidance analysis for scenario 2 (scen2). The orange section represents the successful avoidance (classification = 1), and the blue section represents the failed obstacle avoidance (classification = 0).

4.2 Results Analysis and Comparison

After pertinent analysis, it is observed that the U-RRT* outperforms in all the metrics compared to the other algorithms. First, in the execution time metric, it is observed that there is a significant difference between the RRT algorithm and U-RRT*

with a significance of two stars (**) in scen1 (Figure 18) and three stars (***) (Figure 19) in scen 2. While a significance of four stars (****) in scen1 and scen 2 (Figure18 and 19, respectively) between RRT connect and U-RRT* was noted. This demonstrates that U-RRT* performs faster than RRT and even faster than RRT connect both in dense and non-dense environments, which is not the case for the other algorithms whose execution time increased as the obstacles increased. Also, for the path length algorithm that introduces an idea of how feasible a path is, RRT connect was found to generate the less feasible path, unlike U-RRT* that generated the shortest paths. The significance between these two was thus high both in scen1 and scen2 (**** in both) (figures 8-9). There was no significant difference between the RRT algorithm and U-RRT* algorithm in scen1 and only a one-star (*) significant difference in scen2 for path length.

For scen1 and scen2 of the success rate metric, only U-RRT* always found a path. It is observed that RRT has difficulties finding a path both in dense and non-dense environments (scen2, scen1 respectively) with a success rate of 10% in non-dense and 20% in dense environments. The RRT connect algorithm was good enough in scen1 with a 65% success rate but less competent in scen2 with a drop to a 50% success rate. The U-RRT* maintained high performance in both scenarios with a 100% success rate. For each algorithm and in each trial and scenario, when a path is found, its smoothness was assessed to emphasize the evaluation of the feasibility of the path, as a jerk-free environment is crucial for implementations related to surgery. For that reason, the smoothness metric reflects smoothness results for trials in which a path was found. In scen1, RRT produced either smooth or partially smooth paths in equal percentage (50%), while in scen2, it generated either moderately smooth or stiff paths still in an equal percentage (50%). RRT connect, on the other hand, in scen1 15% off the paths found were moderately smooth and 85% were stiff paths. In scen2, 10% of the paths found are smooth, 30% are moderately smooth, and 60% are stiff, thus, RRT connect performed better in scen2. In scen1, 10% of paths found by U-RRT* were moderately smooth, and 90% were smooth. İn scen2, all the paths found were smooth. The last metric parameter evaluated if the path found correctly avoided obstacles. RRT had an equal percentage for both scenarios (50%). In scen1, only 44% of the paths found by RRT connect avoided the obstacles correctly. In scen2, 40%

avoided the obstacles correctly, which is even lower compared to scen1. The U-RRT* algorithm always avoided the obstacles correctly.

Chapter 5

Discussions and Conclusions

In summary, the performance of each algorithm varied depending on the specific conditions under which it was applied. The standard RRT algorithm demonstrated significant limitations, particularly in low density environments, with success rates as low as 10% and average obstacle avoidance of only 50%. Its tendency towards excessive exploration resulted in longer computation times and frequent failure to find viable paths. While RRT connect showed improved performance over standard RRT, with a success rate of 65% in sparse environment, it still produced suboptimal results in dense environments, where its success rate dropped to 50%, and only 40-44% of paths successfully avoided obstacles. Moreover, a large proportion of its paths were stiff (85% in scen1), highlighting poor smoothness performance. In contrast, the upgraded RRT* significantly outperformed both baseline methods across all evaluation metrics. Upgraded RRT star was significantly faster, with improvements marked by statistical significance ($p < 0.01$ to $p < 0.0001$) across scenarios. It also generated paths that were up to 20-30% shorter than those generated by RRT connect, with high statistical significance (****). Furthermore, it achieved a consistent 100% success rate in both sparse and dense environments, compared to 10-65% for the other methods. Additionally, it produced 90-100% smooth paths, while RRT and RRT connect generated 50-85% stiff or moderately smooth paths. Lastly, it correctly avoided obstacles in 100% of paths, outperforming RRT (50%) and RRT connect (40-44%). These results demonstrate that U-RRT offers a 50-90% relative improvement in success rate, smoothness and obstacle avoidance over the existing algorithms. Overall, this study presents a reliable, efficient, and clinically relevant path-planning solution for robotically assisted surgery. The proposed algorithm enhances both safety and efficiency, potentially reducing preoperative planning time and improving the operational reliability of robotic arms in an anatomically complex environment.

Looking ahead, future research could explore the integration of reinforcement learning techniques into the planning framework, to enhance the algorithm's adaptability and efficiency, enabling it to generate more context-specific and optimised paths in less computational time.

REFERENCES

2019 IEEE/RSJ International Conference on Intelligent Robots and Systems (IROS). (2019). IEEE.

Abu-Dakka, F. J., Rubio, F., Valero, F., & Mata, V. (2013). Evolutionary indirect approach to solving trajectory planning problem for industrial robots operating in workspaces with obstacles. *European Journal of Mechanics, A/Solids*, 42, 210–218. Retrieved from https://doi.org/10.1016/j.euromechsol.2013.05.007

Alkatout, I., O'Sullivan, O., Peters, G., & Maass, N. (2024, January 1). Expanding Robotic-Assisted Surgery in Gynecology Using the Potential of an Advanced Robotic System. *Medicina (Lithuania)*. Multidisciplinary Digital Publishing Institute (MDPI). Retrieved from https://doi.org/10.3390/medicina60010053

Bernardes, M. C., Adorno, B. V., Poignet, P., & Borges, G. A. (2013). Robot-assisted automatic insertion of steerable needles with closed-loop imaging feedback and intraoperative trajectory replanning. *Mechatronics*, 23(6), 630–645. Retrieved from https://doi.org/10.1016/j.mechatronics.2013.06.004

Chakraborty, S., Elangovan, D., Govindarajan, P. L., ELnaggar, M. F., Alrashed, M. M., & Kamel, S. (2022, August 1). A Comprehensive Review of Path Planning for Agricultural Ground Robots. *Sustainability (Switzerland)*. MDPI. Retrieved from https://doi.org/10.3390/su14159156

Chen, Y., Fu, Y., Zhang, B., Fu, W., & Shen, C. (2022). Path planning of the fruit tree pruning manipulator based on improved RRT-Connect algorithm. *International Journal of Agricultural and Biological Engineering*, 15(2), 177–188. Retrieved from https://doi.org/10.25165/j.ijabe.20221502.6249

Cheng, C., Sha, Q., He, B., & Li, G. (2021, September 1). Path planning and obstacle avoidance for AUV: A review. *Ocean Engineering*.

Elsevier Ltd. Retrieved from https://doi.org/10.1016/j.oceaneng.2021.109355

Cheng, Q., Zhang, W., Liu, H., Zhang, Y., & Hao, L. (2021). Research on the path planning algorithm of a manipulator based on gmm/gmr-mprm. *Applied Sciences (Switzerland)*, 11(16). Retrieved from https://doi.org/10.3390/app11167599

Cheng, X., Zhou, J., Zhou, Z., Zhao, X., Gao, J., & Qiao, T. (2023). An improved RRT-Connect path planning algorithm of robotic arm for automatic sampling of exhaust emission detection in Industry 4.0. *Journal of Industrial Information Integration*, 33. Retrieved from https://doi.org/10.1016/j.jii.2023.100436

Cursi, F., & Kormushev, P. (2021). Pre-operative Offline Optimization of Insertion Point Location for Safe and Accurate Surgical Task Execution. In *IEEE International Conference on Intelligent Robots and Systems* (pp. 4040–4047). Institute of Electrical and Electronics Engineers Inc. Retrieved from https://doi.org/10.1109/IROS51168.2021.9636285

Dai, J., Zhang, Y., & Deng, H. (2024). Novel Potential Guided Bidirectional RRT∗With Direct Connection Strategy for Path Planning of Redundant Robot Manipulators in Joint Space. *IEEE Transactions on Industrial Electronics*, 71(3), 2737–2747. Retrieved from https://doi.org/10.1109/TIE.2023.3269462

Delaney, R. A. (2024). The present and future of preoperative planning. *JSES International*. Retrieved from https://doi.org/10.1016/j.jseint.2024.09.002

Demir, G. and R. A. V. (2021). Heuristic Trajectory Planning of Robot Manipulator. In *Heuristic Trajectory Planning of Robot Manipulator* (pp. 222–226). In 2021 IEEE Jordan International Joint Conference on Electrical Engineering and Information Technology (JEEIT). Retrieved from https://doi.org/10.1109/JEEIT53412.2021.9634101

Duan, Y., & Zhang, T. (2022). Energy Optimal Trajectory Algorithm for a Robotic Manipulator. In *Proceedings - 2022 International*

Conference on Artificial Intelligence and Autonomous Robot Systems, AIARS 2022 (pp. 187–191). Institute of Electrical and Electronics Engineers Inc. Retrieved from https://doi.org/10.1109/AIARS57204.2022.00049

Fairchild, P. R., Srivastava, V., & Tan, X. (2021). Efficient Path Planning of Soft Robotic Arms in the Presence of Obstacles. In *IFAC-PapersOnLine* (Vol. 54, pp. 586–591). Elsevier B.V. Retrieved from https://doi.org/10.1016/j.ifacol.2021.11.235

Gao, Q., Yuan, Q., Sun, Y., & Xu, L. (2023). Path planning algorithm of robot arm based on improved RRT* and BP neural network algorithm. *Journal of King Saud University - Computer and Information Sciences*, 35(8). Retrieved from https://doi.org/10.1016/j.jksuci.2023.101650

Hao, L., Liu, D., Du, S., Wang, Y., Wu, B., Wang, Q., & Zhang, N. (2022). An improved path planning algorithm based on artificial potential field and primal-dual neural network for surgical robot. *Computer Methods and Programs in Biomedicine*, 227. Retrieved from https://doi.org/10.1016/j.cmpb.2022.107202

Hügle, S., Genc, E., Dittmann, J., & Middendorf, P. (2022). Offline Robot-Path-Planning and Process Simulation for the Structural Analysis of Coreless Wound Fibre-Polymer Composite Structures. In *Key Engineering Materials* (Vol. 926 KEM, pp. 1445–1453). Trans Tech Publications Ltd. Retrieved from https://doi.org/10.4028/p-970esd

Jayanthi, S., Chen, L., Balabanska, N., Duong, V., Scarlatescu, E., Ameperosa, E., … Gombolay, M. (n.d.). *DROID: Learning from Offline Heterogeneous Demonstrations via Reward-Policy Distillation*.

Ji, G., Gao, Q., Zhang, T., Cao, L., & Sun, Z. (2023). A Heuristically Accelerated Reinforcement Learning-Based Neurosurgical Path Planner. *Cyborg and Bionic Systems*, 4. Retrieved from https://doi.org/10.34133/CBSYSTEMS.0026

Ji, H., Xie, H., Wang, C., & Yang, H. (2023). E-RRT*: Path Planning for Hyper-Redundant Manipulators. *IEEE Robotics and Automation Letters*, 8(12), 8128–8135. Retrieved from https://doi.org/10.1109/LRA.2023.3325716

Jiang, L., Liu, S., Cui, Y., & Jiang, H. (2022). Path Planning for Robotic Manipulator in Complex Multi-Obstacle Environment Based on Improved_RRT. *IEEE/ASME Transactions on Mechatronics*, 27(6), 4774–4785. Retrieved from https://doi.org/10.1109/TMECH.2022.3165845

Kang, J. G., Lim, D. W., Choi, Y. S., Jang, W. J., & Jung, J. W. (2021). Improved RRT-connect algorithm based on triangular inequality for robot path planning. *Sensors (Switzerland)*, 21(2), 1–34. Retrieved from https://doi.org/10.3390/s21020333

Kisinde, S., Hu, X., Hesselbacher, S., & Lieberman, I. H. (2021). The predictive accuracy of surgical planning using pre-op planning software and a robotic guidance system. *European Spine Journal*, 30(12), 3676–3687. Retrieved from https://doi.org/10.1007/s00586-021-06942-w

Lin, H., Xie, Y., Wang, Z., & Wang, S. (2023). A Deep Reinforcement Learning Approach for Pre-Planning Problems in Robotic Intra-Operative Ultrasound: a Virtual Environment-Based Analysis. In *2023 IEEE 3rd International Conference on Digital Twins and Parallel Intelligence, DTPI 2023*. Institute of Electrical and Electronics Engineers Inc. Retrieved from https://doi.org/10.1109/DTPI59677.2023.10365457

Liu, X. S., & Cao, L. (2022). Simulation of Manipulator Path Planning Based on Improved RRT∗ Algorithm. In *2022 5th International Conference on Pattern Recognition and Artificial Intelligence, PRAI 2022* (pp. 1115–1120). Institute of Electrical and Electronics Engineers Inc. Retrieved from https://doi.org/10.1109/PRAI55851.2022.9904064

Long, H., Li, G., Zhou, F., & Chen, T. (2023). Cooperative Dynamic Motion Planning for Dual Manipulator Arms Based on RRT*Smart-

AD Algorithm. *Sensors*, 23(18). Retrieved from https://doi.org/10.3390/s23187759

Manrique-Cordoba, J., Martorell, C., Romero-Ante, J. D., & Sabater-Navarro, J. M. (2024). Neural Tract Avoidance Path-Planning Optimization: Robotic Neurosurgery. *Applied Sciences (Switzerland)*, 14(9). Retrieved from https://doi.org/10.3390/app14093687

Massaro, M., Lovato, S., Bottin, M., & Rosati, G. (2023). An Optimal Control Approach to the Minimum-Time Trajectory Planning of Robotic Manipulators. *Robotics*, 12(3). Retrieved from https://doi.org/10.3390/robotics12030064

Mohammed, H., Romdhane, L., & Jaradat, M. A. (2021). RRT*N: an efficient approach to path planning in 3D for Static and Dynamic Environments. *Advanced Robotics*, 35(3–4), 168–180. Retrieved from https://doi.org/10.1080/01691864.2020.1850349

Monfaredi, R., Concepcion-Gonzalez, A., Acosta Julbe, J., Fischer, E., Hernandez-Herrera, G., Cleary, K., & Oluigbo, C. (2024, August 1). Automatic Path-Planning Techniques for Minimally Invasive Stereotactic Neurosurgical Procedures—A Systematic Review. *Sensors*. Multidisciplinary Digital Publishing Institute (MDPI). Retrieved from https://doi.org/10.3390/s24165238

Noreen, I., Khan, A., & Habib, Z. (2016). *A Comparison of RRT, RRT* and RRT*-Smart Path Planning Algorithms*. *IJCSNS International Journal of Computer Science and Network Security* (Vol. 16).

Pan, Z., Zhang, C., Xia, Y., Xiong, H., & Shao, X. (2022). An Improved Artificial Potential Field Method for Path Planning and Formation Control of the Multi-UAV Systems. *IEEE Transactions on Circuits and Systems II: Express Briefs*, 69(3), 1129–1133. Retrieved from https://doi.org/10.1109/TCSII.2021.3112787

Rajendran, P., Thakar, S., Bhatt, P. M., Kabir, A. M., & Gupta, S. K. (2021). Strategies for Speeding Up Manipulator Path Planning to Find High Quality Paths in Cluttered Environments. *Journal of*

Computing and Information Science in Engineering, 21(1). Retrieved from https://doi.org/10.1115/1.4048619

Robot Arm Path Planning Based on Improved RRT. (n.d.).

Ryan Luna, I. A. S. M. M. and L. E. K. (2013). 2013 IEEE International Conference on Robotics and Automation. In *Anytime Solution Optimization for Sampling-Based Motion Planning* (pp. 5068–5074). IEEE International Conference on Robotics and Automation (ICRA).

Santos, R. R., Rade, D. A., & da Fonseca, I. M. (2022). A machine learning strategy for optimal path planning of space robotic manipulator in on-orbit servicing. *Acta Astronautica*, 191, 41–54. Retrieved from https://doi.org/10.1016/j.actaastro.2021.10.031

Segato, A., Marzo, M. Di, Zucchelli, S., Galvan, S., Secoli, R., & De Momi, E. (2022). Inverse Reinforcement Learning Intra-Operative Path Planning for Steerable Needle. *IEEE Transactions on Biomedical Engineering*, 69(6), 1995–2005. Retrieved from https://doi.org/10.1109/TBME.2021.3133075

Shao, J., Xiong, H., Liao, J., Song, W., Chen, Z., Gu, J., & Zhu, S. (2021). RRT-GoalBias and path smoothing based motion planning of mobile manipulators with obstacle avoidance. In *2021 IEEE International Conference on Real-Time Computing and Robotics, RCAR 2021* (pp. 217–222). Institute of Electrical and Electronics Engineers Inc. Retrieved from https://doi.org/10.1109/RCAR52367.2021.9517335

Shen, H., Xie, W. F., Tang, J., & Zhou, T. (2023). Adaptive Manipulability-Based Path Planning Strategy for Industrial Robot Manipulators. *IEEE/ASME Transactions on Mechatronics*, 28(3), 1742–1753. Retrieved from https://doi.org/10.1109/TMECH.2022.3231467

Shen, Y., Liu, J., & Luo, Y. (2021). Review of Path Planning Algorithms for Unmanned Vehicles. In *Proceedings of 2021 IEEE 2nd International Conference on Information Technology, Big Data and Artificial Intelligence, ICIBA 2021* (pp. 400–405). Institute of

Electrical and Electronics Engineers Inc. Retrieved from https://doi.org/10.1109/ICIBA52610.2021.9688064

Shi, W., Wang, K., Zhao, C., & Tian, M. (2022). Obstacle Avoidance Path Planning for the Dual-Arm Robot Based on an Improved RRT Algorithm. *Applied Sciences (Switzerland)*, 12(8). Retrieved from https://doi.org/10.3390/app12084087

Song, Q., Li, S., Bai, Q., Yang, J., Zhang, A., Zhang, X., & Zhe, L. (2021). Trajectory planning of robot manipulator based on rbf neural network. *Entropy*, 23(9). Retrieved from https://doi.org/10.3390/e23091207

Su, Hang, Jamal Sheiban, F., Qi, W., Salih Ovur, E., & Alfayad, S. (2024). A Bioinspired Virtual Reality Toolkit for Robot-Assisted Medical Application: BioVRbot. *IEEE Transactions on Human-Machine Systems*. Retrieved from https://doi.org/10.1109/THMS.2024.3462416

Su, Hao, Kwok, K. W., Cleary, K., Iordachita, I., Cavusoglu, M. C., Desai, J. P., & Fischer, G. S. (2022). State of the Art and Future Opportunities in MRI-Guided Robot-Assisted Surgery and Interventions. *Proceedings of the IEEE*, 110(7), 968–992. Retrieved from https://doi.org/10.1109/JPROC.2022.3169146

Sundaram, A. M., Budjakoski, N., Klodmann, J., & Roa, M. A. (2022). Task-specific robot base pose optimization for robot-assisted surgeries. *Frontiers in Robotics and AI*, 9. Retrieved from https://doi.org/10.3389/frobt.2022.899646

Tavares, R. S., Martins, T. C., & Tsuzuki, M. S. G. (2011). Simulated annealing with adaptive neighborhood: A case study in off-line robot path planning. *Expert Systems with Applications*, 38(4), 2951–2965. Retrieved from https://doi.org/10.1016/j.eswa.2010.08.084

Thamo, B., Voulgaridou, V., Wood, H., Stone, J., Dhaliwal, K., & Khadem, M. (2024). Toward Robotics-Assisted Endomicroscopy in Percutaneous Needle-Based Interventions. *IEEE Transactions on Medical Robotics and Bionics*, 6(1), 110–119. Retrieved from https://doi.org/10.1109/TMRB.2023.3337869

Tian, L., Zhang, Z., Zheng, C., Tian, Y., Zhao, Y., Wang, Z., & Qin, Y. (2021). An improved rapidly-exploring random trees algorithm combining parent point priority determination strategy and real-time optimization strategy for path planning. *Sensors*, 21(20). Retrieved from https://doi.org/10.3390/s21206907

Towards Comparison and Real Time Implementation of Path Planning Methods for 2R Planar Manipulator with Obstacles Avoidance. . (n.d.).

Tzanetis, P., Fluit, R., de Souza, K., Robertson, S., Koopman, B., & Verdonschot, N. (2023). Pre-Planning the Surgical Target for Optimal Implant Positioning in Robotic-Assisted Total Knee Arthroplasty. *Bioengineering*, 10(5). Retrieved from https://doi.org/10.3390/bioengineering10050543

Wang, J., Zhao, Z., Liang, H., Zhang, R., Liu, X., Zhang, J., … Yang, R. (2024). Artificial intelligence assisted preoperative planning and 3D-printing guiding frame for percutaneous screw reconstruction in periacetabular metastatic cancer patients. *Frontiers in Bioengineering and Biotechnology*, 12. Retrieved from https://doi.org/10.3389/fbioe.2024.1404937

Wang, R., Xie, Y., Chen, X., & Li, Y. (2023). Path-Constrained Time-Optimal Motion Planning for Robot Manipulators With Third-Order Constraints. *IEEE/ASME Transactions on Mechatronics*, 28(6), 3005–3016. Retrieved from https://doi.org/10.1109/TMECH.2023.3234584

Wang, Y., Tian, J., Liu, Z., Liu, H., Liu, J., & Xie, L. (2022). Path planning of manipulator based on improved RRT algorithm. In *Journal of Physics: Conference Series* (Vol. 2216). IOP Publishing Ltd. Retrieved from https://doi.org/10.1088/1742-6596/2216/1/012012

Weber, A. M., Gambao, E., & Brunete, A. (2023). A Survey on Autonomous Offline Path Generation for Robot-Assisted Spraying Applications. *Actuators*, 12(11). Retrieved from https://doi.org/10.3390/act12110403

Wei, H., Zheng, Y., & Gu, G. (2021). RRT-Based Path Planning for Follow-the-Leader Motion of Hyper-Redundant Manipulators. In *IEEE International Conference on Intelligent Robots and Systems* (pp. 3198–3204). Institute of Electrical and Electronics Engineers Inc. Retrieved from https://doi.org/10.1109/IROS51168.2021.9635876

Wen, Yalun, & Pagilla, P. (2023). Path-Constrained and Collision-Free Optimal Trajectory Planning for Robot Manipulators. *IEEE Transactions on Automation Science and Engineering*, 20(2), 763–774. Retrieved from https://doi.org/10.1109/TASE.2022.3169989

Wen, Yang, Haiying, W., & Zhisheng, Z. (2021). Obstacle Avoidance Path Planning of Manipulator Based on Improved RRT Algorithm. In *2021 International Conference on Computer, Control and Robotics, ICCCR 2021* (pp. 104–109). Institute of Electrical and Electronics Engineers Inc. Retrieved from https://doi.org/10.1109/ICCCR49711.2021.9349398

Xu, J., & Wang, J. (2022). Effective motion planning of manipulator based on SDPS-RRTConnect. *Robotica*, 40(6), 1855–1867. Retrieved from https://doi.org/10.1017/S0263574721001417

Xu, T. (2024, June 15). Recent advances in Rapidly-exploring random tree: A review. *Heliyon*. Elsevier Ltd. Retrieved from https://doi.org/10.1016/j.heliyon.2024.e32451

Yang, H., Li, H., Liu, K., Yu, W., & Li, X. (2021). Research on path planning based on improved RRT-Connect algorithm. In *Proceedings of the 33rd Chinese Control and Decision Conference, CCDC 2021* (pp. 5707–5712). Institute of Electrical and Electronics Engineers Inc. Retrieved from https://doi.org/10.1109/CCDC52312.2021.9602203

Yao, J. (2024). RRT algorithm learning and optimization. *Applied and Computational Engineering*, 53(1), 296–302. Retrieved from https://doi.org/10.54254/2755-2721/53/20241614

Yi, J., Yuan, Q., Sun, R., & Bai, H. (2022). Path planning of a manipulator based on an improved P_RRT* algorithm. *Complex*

and Intelligent Systems, 8(3), 2227–2245. Retrieved from https://doi.org/10.1007/s40747-021-00628-y

Yu, X., Dong, M., & Yin, W. (2022). Time-optimal trajectory planning of manipulator with simultaneously searching the optimal path. *Computer Communications*, 181, 446–453. Retrieved from https://doi.org/10.1016/j.comcom.2021.10.005

Yu, Y. H., & Zhang, Y. T. (2022). Collision avoidance and path planning for industrial manipulator using slice-based heuristic fast marching tree. *Robotics and Computer-Integrated Manufacturing*, 75. Retrieved from https://doi.org/10.1016/j.rcim.2021.102289

Yuan, Q., Yi, J., Sun, R., & Bai, H. (2021). Path planning of a mechanical arm based on an improved artificial potential field and a rapid expansion random tree hybrid algorithm. *Algorithms*, 14(11). Retrieved from https://doi.org/10.3390/a14110321

Zhang, H., Zhu, L., Shen, J., & Song, A. (2023). Implicit Neural Field Guidance for Teleoperated Robot-assisted Surgery. In *Proceedings - IEEE International Conference on Robotics and Automation* (Vol. 2023-May, pp. 6866–6872). Institute of Electrical and Electronics Engineers Inc. Retrieved from https://doi.org/10.1109/ICRA48891.2023.10160475

Zhang, Q., Liu, F., & Li, B. (2023). A heuristic tomato-bunch harvest manipulator path planning method based on a 3D-CNN-based position posture map and rapidly-exploring random tree. *Computers and Electronics in Agriculture*, 213. Retrieved from https://doi.org/10.1016/j.compag.2023.108183

Zhang, Y., Ju, Z., Zhang, H., & Qi, Z. (2022). 3-D Path Planning Using Improved RRT∗ Algorithm for Robot-Assisted Flexible Needle Insertion in Multilayer Tissues. *IEEE Canadian Journal of Electrical and Computer Engineering*, 45(1), 50–62. Retrieved from https://doi.org/10.1109/ICJECE.2021.3120324

Zhao, Z., Jiang, Y., Bales, C., Wang, Y., & Fischer, G. (2024). Development of Advanced FEM Simulation Technology for Pre-

Operative Surgical Planning. Retrieved from http://arxiv.org/abs/2409.03990

Zhong, J., Wang, T., & Cheng, L. (2022). Collision-free path planning for welding manipulator via hybrid algorithm of deep reinforcement learning and inverse kinematics. *Complex and Intelligent Systems*, 8(3), 1899–1912. Retrieved from https://doi.org/10.1007/s40747-021-00366-1

Zhuang, M., Li, G., & Ding, K. (2023). Obstacle Avoidance Path Planning for Apple Picking Robotic Arm Incorporating Artificial Potential Field and A∗Algorithm. *IEEE Access*, 11, 100070–100082. Retrieved from https://doi.org/10.1109/ACCESS.2023.3312763

LIU Yaqiu, Z. H. L. X. X. Y. (2021). *An Improved RRT Based Obstacle Avoidance Path Planning Algorithm for Industrial Robot*.